

Article

Phosphorylation of CENP-R by Aurora B regulates kinetochore–microtubule attachment for accurate chromosome segregation

Divine Mensah Sedzro^{1,2}, Xiao Yuan^{1,2,*}, McKay Mullen^{1,2,3}, Umer Ejaz^{1,2}, Tongtong Yang^{1,2}, Xu Liu^{1,2,3}, Xiaoyu Song^{1,2,3}, Yun-Chi Tang⁴, Weijun Pan⁴, Peng Zou⁵, Xinjiao Gao^{1,2}, Dongmei Wang^{1,2}, Zhikai Wang^{1,2,3}, Zhen Dou^{1,2,*}, Xing Liu^{1,2,3,*}, and Xuebiao Yao^{1,2,*}

¹ MOE Key Laboratory for Cellular Dynamics, University of Science and Technology of China School of Life Sciences, Hefei 230027, China

² Anhui Key Laboratory for Cellular Dynamics and Chemical Biology, National Center for Cross-Disciplinary Sciences & CAS Center for Excellence in Molecular Cell Science, Hefei 230026, China

³ Morehouse School of Medicine, Atlanta, GA 30310, USA

⁴ Shanghai Institute of Nutrition and Health, Shanghai Institutes for Biological Sciences, Chinese Academy of Sciences (CAS), Shanghai 200031, China

⁵ College of Chemistry and Molecular Engineering, Peking University, Beijing 100871, China

* Correspondence to: Xiao Yuan, E-mail: yuanxiao@ustc.edu.cn; Zhen Dou, E-mail: douzhen@ustc.edu.cn; Xing Liu, E-mail: xing1017@ustc.edu.cn; Xuebiao Yao, E-mail: yaoxb@ustc.edu.cn

Edited by Jiarui Wu

Error-free mitosis depends on accurate chromosome attachment to spindle microtubules via a fine structure called the centromere that is epigenetically specified by the enrichment of CENP-A nucleosomes. Centromere maintenance during mitosis requires CENP-A-mediated deposition of constitutive centromere-associated network that establishes the inner kinetochore and connects centromeric chromatin to spindle microtubules during mitosis. Although previously proposed to be an adaptor of retinoic acid receptor, here, we show that CENP-R synergizes with CENP-OPQU to regulate kinetochore–microtubule attachment stability and ensure accurate chromosome segregation in mitosis. We found that a phospho-mimicking mutation of CENP-R weakened its localization to the kinetochore, suggesting that phosphorylation may regulate its localization. Perturbation of CENP-R phosphorylation is shown to prevent proper kinetochore–microtubule attachment at metaphase. Mechanistically, CENP-R phosphorylation disrupts its binding with CENP-U. Thus, we speculate that Aurora B-mediated CENP-R phosphorylation promotes the correction of improper kinetochore–microtubule attachment in mitosis. As CENP-R is absent from yeast, we reasoned that metazoan evolved an elaborate chromosome stability control machinery to ensure faithful chromosome segregation in mitosis.

Keywords: constitutive centromere-associated network (CCAN), kinetochore, microtubule, Aurora B, CENP-R, phosphorylation

Introduction

Correct chromosome segregation depends on a unique chromatin domain known as the centromere, which is a specialized chromatin domain present throughout the cell cycle and acts as a platform on which the transient assembly of the kinetochore occurs during mitosis (Cleveland et al., 2003; McKinley and Cheeseman, 2016; Liu et al., 2020). The kinetochore is one of

the most sophisticated molecular machineries for cell division in eukaryotic cells and forms a dynamic link between spindle microtubule attachment and quality control of the spindle assembly checkpoint (SAC), a signaling cascade that prevents chromosome segregation before completion of bi-orientation during cell division (Kops et al., 2020).

The centromere is built on the specific foundation called CENP-A nucleosome and the constitutive centromere-associated network (CCAN) that is organized into different stable sub-complexes (Foltz et al., 2006; Okada et al., 2006; Hori et al., 2008). CENP-C and other CCAN subunits, such as CENP-T, also provide a platform for the assembly of the kinetochore's outer layer (Hori et al., 2008; Gascoigne et al., 2011; Schleiffer et al., 2012). The outer kinetochore comprises three further

Received January 27, 2022. Revised June 14, 2022. Accepted September 1, 2022.
© The Author(s) (2022). Published by Oxford University Press on behalf of *Journal of Molecular Cell Biology*, CEMCS, CAS.

This is an Open Access article distributed under the terms of the Creative Commons Attribution-NonCommercial License (<https://creativecommons.org/licenses/by-nc/4.0/>), which permits non-commercial re-use, distribution, and reproduction in any medium, provided the original work is properly cited. For commercial re-use, please contact journals.permissions@oup.com

sub-complexes, known as the KNL1, MIS12, and NDC80 complexes, and collectively referred to as the KMN network (Cheeseman and Desai, 2008). Besides important regulatory functions, the KMN network, through its NDC80 complex, provides a site for binding with spindle microtubules, an interaction that promotes the alignment and segregation of chromosomes to the daughter cells (Musacchio and Desai, 2017).

The overall architecture of budding yeast CCAN was described previously (Yan et al., 2019). Our recent structural analyses, together with two other independent studies, show that the global architecture of human CCAN has significant similarity with yeast CCAN (Pesenti et al., 2022; Tian et al., 2022; Yatskevich et al., 2022). Nevertheless, a fundamental difference is that human CCAN topologically entraps CENP-A nucleosome linker DNA. Given the metazoan centromere evolution (Wang et al., 2004; Liu et al., 2020), the precise function of certain human CCAN components could not be inferred from yeast CCAN structure and activity relationship studies. For example, CENP-R is absent from yeast and was known as nuclear receptor-interacting factor-3 and perturbation of its function alters the cell fate decision (Li et al., 1999; Li et al., 2001). Centromere proteomic analyses identified CENP-R as an integral component of CENP-A nucleosome distal complex, which is essential for prevention of premature sister chromatid separation during recovery from spindle damage (Foltz et al., 2006; Hori et al., 2008; Cao et al., 2021). However, the precise interaction of CENP-R with its relation to the CENP-OPQU complex, in particular, how CENP-R functions in chromosome segregation in mitosis, remains elusive.

In this study, we identified CENP-R as a *bona fide* substrate of Aurora B. Persistent expression of phospho-mimetic CENP-R-S28D mutant causes massive chromosome misalignment, while the non-phosphorylatable CENP-R-S28A mutant results in elevated proportion of cells with chromosome alignment defects. Mechanistically, persistent CENP-R phosphorylation by Aurora B destabilizes kinetochore–microtubule attachment because of disrupted CENP-U–CENP-R binding. Our studies reveal how dynamic phosphorylation of CENP-R ensures accurate chromosome segregation and sister chromatid separation.

Results

Characterization of the structural determinant for CENP-R localization to the kinetochore

CENP-OPQUR is a sub-complex of the CCAN machinery localized to the kinetochore during mitosis. However, the structural determinant for CENP-R localization to the kinetochore has remained elusive due to its intrinsically disordered region. First, we verified the kinetochore localization of CENP-R via immunofluorescence staining using a commercial CENP-R antibody. Consistent with the previous study (Foltz et al., 2006), CENP-R localized at the kinetochore throughout the cell cycle (Figure 1A). We next set out to determine the minimum region of CENP-R required for its centromere location. To this end, we designed plasmids expressing different truncations of CENP-R. Since the structure of full-length CENP-R was unknown, we utilized the predicted secondary structure as a guide in designing

the truncations to avoid disrupting the secondary structure of CENP-R. However, CENP-R aa81–160 is a continuous coiled-coil fragment according to AlphaFold prediction (Figure 1B). Then, we transiently expressed the GFP-tagged protein in HeLa cells and analyzed its localization by indirect immunofluorescence microscopy. As shown in Figure 1C, the CENP-R C-terminus (aa81–160) localized to the centromere as strong as the CENP-R full-length (FL) in mitotic cells, indicating that the region containing aa81–160 is the determinant of CENP-R localization to the centromere. Neither the N-terminal (aa1–80) nor deletion mutants (aa1–140 and aa101–177) could localize at the kinetochore (Figure 1C). Statistical analyses of immunofluorescence intensity of CENP-R-GFP and the deletion mutants concluded that the region containing aa81–160 is the determinant of CENP-R localization to the kinetochore (Figure 1D).

CENP-R is essential for accurate chromosome segregation

The successful determination of CENP-R localization signal prompted us to survey the temporal dynamics of CENP-R protein expression profile during the cell cycle. We next assessed the temporal profile of CENP-R levels during mitosis relative to those of cyclin B1 and tubulin by collecting synchronized HeLa cells for western blotting. CENP-R expression profile was different from that of cyclin B1, as the level of CENP-R was rather persistent during cell cycle (Figure 2A). To systemically assess the functional relevance of CENP-R in chromosome segregation, we utilized three independent shRNAs to suppress CENP-R protein level according to previous work (Pesenti et al., 2018). To optimize the transfection efficiency, the shRNAs were packaged into lentiviruses and used to infect the cells. Trial experiments were carried out to determine the efficiency of the three independent shRNAs for suppressing CENP-R protein level. As shown in Figure 2B, the shCENP-R #3 exhibited the best efficiency in suppressing CENP-R protein as judged by western blotting. The shCENP-R #3 was therefore selected for this study and referred to as shCENP-R. Interestingly, depletion of CENP-R resulted in mitotic defects such as chromosome misalignment and multipolar spindle (Figure 2C). Statistical analyses from three independent experiments showed that chromosome misalignment phenotype is a hallmark of CENP-R suppression (Figure 2D). The SAC, an internal surveillance signaling mechanism, prevents the cells from entering anaphase until all kinetochores are properly attached to the microtubules (van der Waal et al., 2012; Lara-Gonzalez et al., 2021). Mps1 is an important kinase involved in the spindle checkpoint activation, and inhibition of Mps1 kinase activity through small-molecule inhibitors, such as reversine, renders the SAC ineffective resulting in cells bypassing metaphase during mitosis with aberrations in chromosome segregation (Meraldi et al., 2004; Santaguida et al., 2010; Dou et al., 2015; Gui et al., 2020). Due to the chronic arrest in near-metaphase observed in HeLa cells upon depletion of endogenous CENP-R (Figure 2C, middle panel), we speculated that CENP-R depletion may cause SAC activation. For this purpose, we applied 0.5 μ M reversine to HeLa cells depleted of CENP-R and the cells were arrested in near-metaphase for at least 1 h.

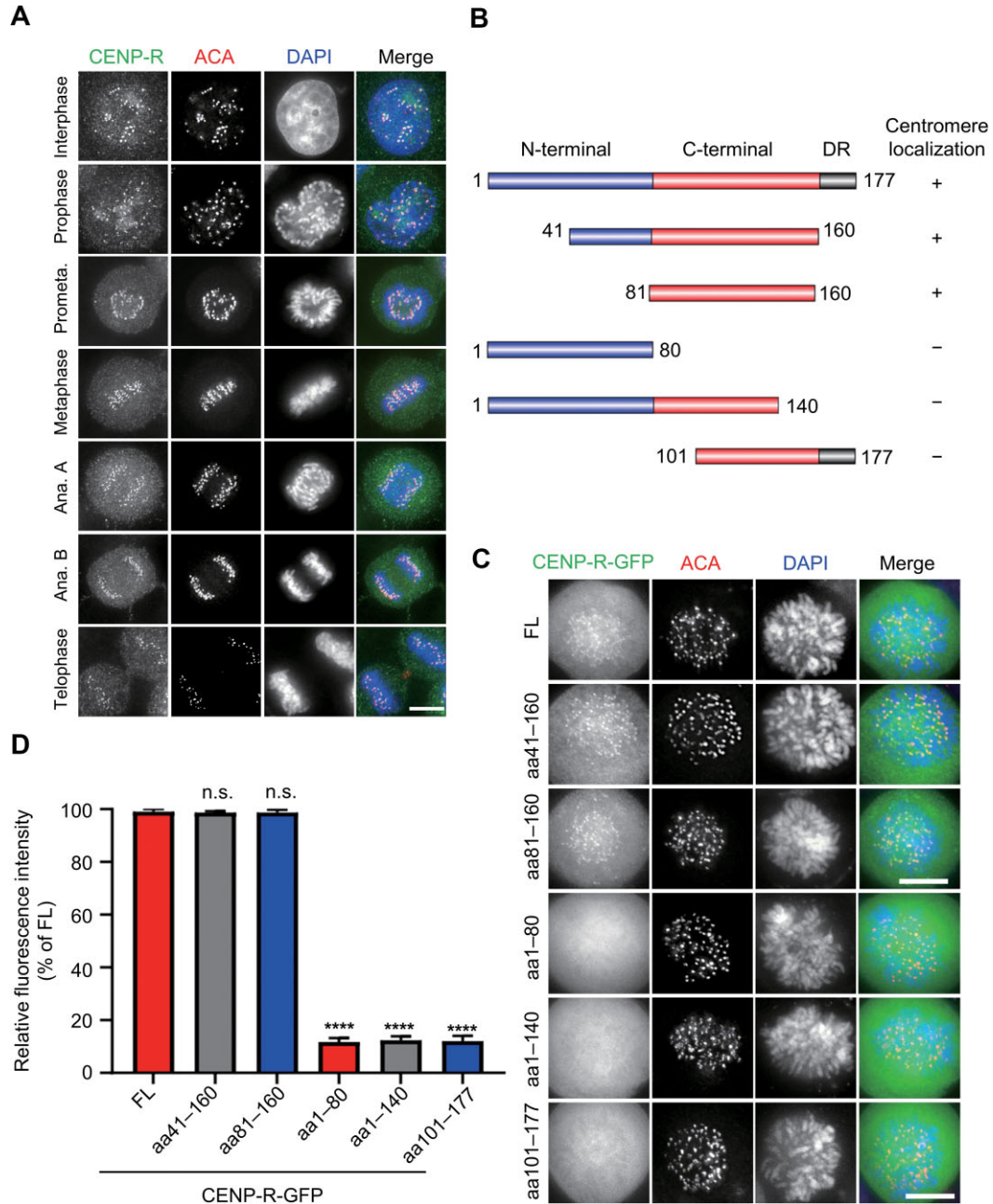


Figure 1 Characterization of centromere localization determinant of CENP-R. **(A)** Subcellular localization of endogenous CENP-R during cell cycle. This montage represents optical images collected from HeLa cells that are triply-stained for the centromere marker ACA (red), CENP-R (green), and DAPI (blue). Scale bar, 10 μ m. **(B)** Schematic drawing of CENP-R deletion mutants for identification of centromere localization determinant. +, positive for centromere localization; -, negative for centromere localization. **(C)** C-terminus of CENP-R (aa81-160) is sufficient for stable localization to the centromere. HeLa cells were transfected with full-length (FL) CENP-R and the deletion mutants. At 48 h post transfection, cells were fixed and stained for ACA (red) and DAPI (blue). Scale bar, 10 μ m. **(D)** Quantification of the centromere localization for the CENP-R constructs as illustrated in **C**. A total of 50 mitotic cells expressing CENP-R-GFP or the deletion mutants from three separate experiments were surveyed. Statistical significance was tested by two-sided *t*-test and represented by **** $P < 0.0001$; n.s., not significant. $n = 3$. Bars indicate mean \pm SD.

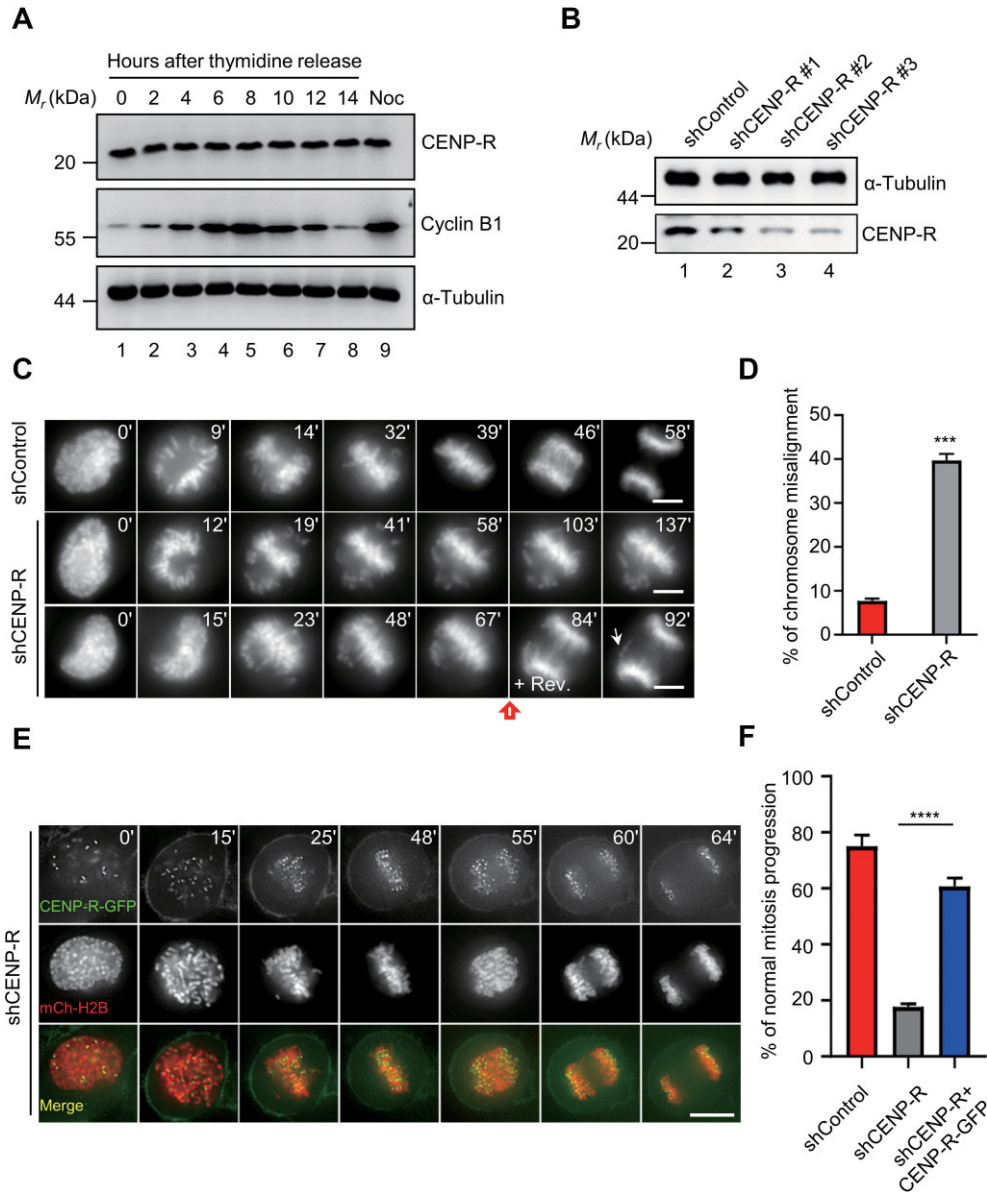


Figure 2 Depletion of CENP-R causes mitotic defects. **(A)** Cell cycle expression profile of CENP-R. Western blotting analyses of CENP-R in synchronized HeLa cells. Note that the level of CENP-R is relatively stable, while cyclin B levels change from interphase to mitosis. **(B)** Characterization of the efficiency of shRNA for CENP-R knockdown. Western blotting analyses of CENP-R protein level after transfection of three independent CENP-R shRNAs. **(C)** Suppression of CENP-R causes mitotic defects. HeLa cells were transfected with shCENP-R #3 along with mCherry-H2B as a marker of chromosome DNA. At 24 h post transfection, cells were synchronized for real-time imaging. An aliquot of reversine (0.5 μ M) was applied to cells arrested at metaphase (red arrow) for > 1 h during real-time experiments. Time is indicated in minutes. Scale bar, 10 μ m. **(D)** Quantification of chromosome misalignment phenotype in C. An average of 50 GFP- and mCherry-positive mitotic cells from three separate experiments were surveyed. Statistical significance was tested by two-sided *t*-test and represented by *** $P < 0.001$ and **** $P < 0.0001$; $n = 3$. Bars indicate mean \pm SD. **(E)** Expression of CENP-R rescues ShCENP-R-elicited phenotypes. HeLa cells were transfected with shCENP-R #3 along with shRNA-resistant CENP-R-GFP and mCherry-H2B and examined for real-time chromosome dynamics. At 24 h post transfection, cells were synchronized for real-time imaging. Time is indicated in minutes. Scale bar, 10 μ m. **(F)** Bar graph illustrating the percentage of normal mitotic cells in the three indicated groups. Statistical significance was tested by two-sided *t*-test and represented by **** $P < 0.0001$; $n = 3$. Bars indicate mean \pm SD.

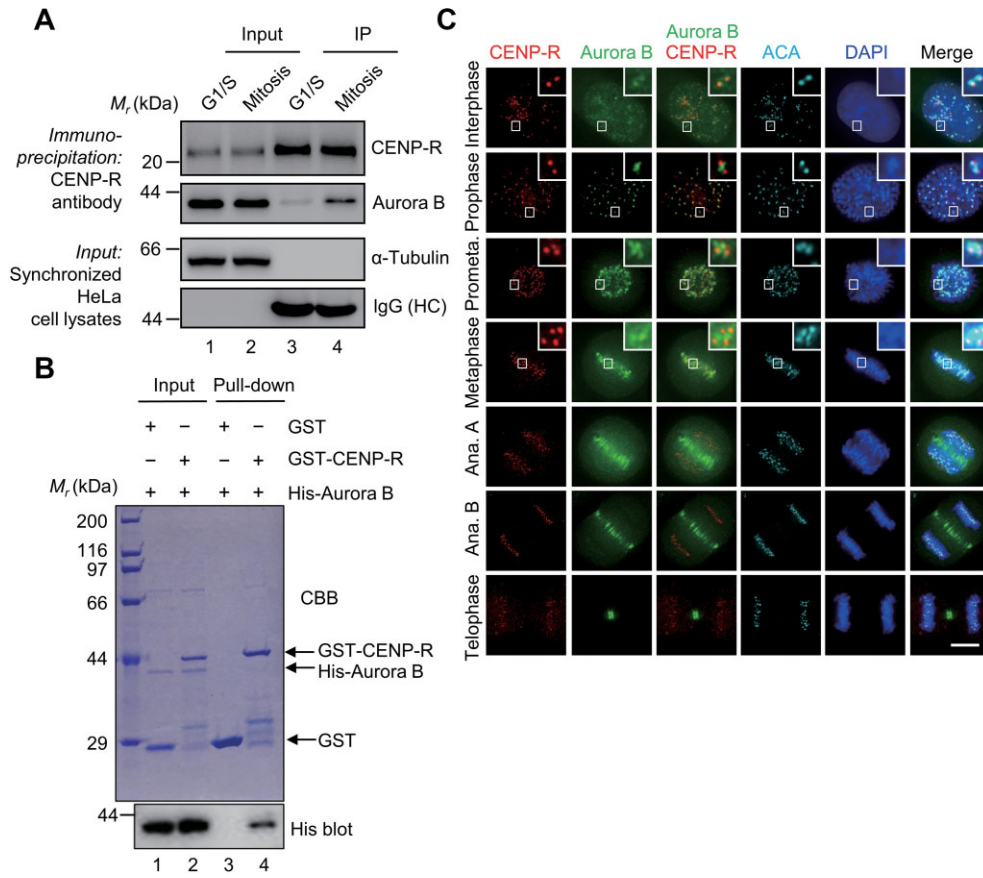


Figure 3 Identification and characterization of a novel CENP-R–Aurora B interaction. **(A)** Endogenous CENP-R immunoprecipitates from interphase and mitotic HeLa cells were detected with antibodies against CENP-R, Aurora B, and tubulin. **(B)** *In vitro* pull-down of His-Aurora B (full length) by GST or GST-CENP-R. The gel was stained with Coomassie Brilliant Blue (CBB) (upper panel). The binding fraction was detected by western blotting analysis with anti-His antibody (lower panel). **(C)** Subcellular localizations of endogenous CENP-R and Aurora B during cell cycle. This montage represents optical images collected from HeLa cells stained for CENP-R (red), Aurora B (green), ACA (cyan), and DAPI (blue). Scale bar, 10 μ m.

As shown in [Figure 2C](#) (bottom panel, red arrow), cells treated with reversine proceeded to divide within 30 min with defects (white arrow). The release indicates that the SAC was activated in the absence of CENP-R. In all, we propose that CENP-R depletion causes chronic SAC activation. To ensure that the phenotypes we observed were not due to off-target effects, a rescue experiment was carried out using shRNA-resistant CENP-R-GFP, which restored accurate chromosome segregation ([Figure 2E](#) and [F](#)). Thus, CENP-R is crucial for proper mitotic progression.

CENP-R interacts with Aurora B *in vitro*

To study the molecular association of CENP-R with other accessory proteins, we carried out an affinity isolation of the CENP-R-containing protein complex followed by mass spectrometric identification of tryptic peptides that are derived from the complex as described previously ([Dransfield et al., 1997](#); [Fang et al., 2006](#); [Ding et al., 2010](#)). Specifically, immunoprecipitates that were isolated from mitotically synchronized HeLa cells expressing CENP-R-GFP or GFP alone, by GFP affinity matrix, were applied to mass spectrometric analyses. Among the identified

proteins that are specific to the CENP-R immunoprecipitate, Aurora B, a characterized mitotic kinase orchestrating accurate kinetochore microtubule attachment to the centromere ([Carmena et al., 2012](#)), ranked together with other known CCAN components (Supplementary Tables S1, S2, and [Figure S1A](#)). Western blotting analyses validated that Aurora B indeed exists in huge amount in the CENP-R immunoprecipitates of mitotic HeLa cells ([Figure 3A](#), lane 4), but less in HeLa cells in G1/S phase ([Figure 3A](#), lane 3). Tubulin (alpha) was absent from the CENP-R immunoprecipitates of both mitotic and interphase cell lysates, which highlights the specific association between CENP-R and Aurora B. To examine whether Aurora B directly interacts with CENP-R, we carried out a pull-down assay using bacterially expressed recombinant GST-CENP-R as an affinity matrix to absorb purified 6 \times His-tagged Aurora B. As shown in [Figure 3B](#), Aurora B bound to GST-CENP-R but not GST tag (lane 3 vs. lane 4). In addition, exogenously expressed Flag-Aurora B precipitated with CENP-R-GFP ([Supplementary Figure S1B](#)). The observed biochemical interaction between CENP-R and Aurora B prompted us to examine their spatiotemporal distribution relationship

in HeLa cells. As shown in [Figure 3C](#), CENP-R co-localized with anti-centromere antibody (ACA) signal in interphase cells, indicating that CENP-R is a constitutive centromere protein. As nuclear envelope broke down, Aurora B was readily apparent in prophase centromere locating between two CENP-R double-dots ([Figure 3C](#), insets). Their localization pattern persisted from prometaphase to metaphase before Aurora B was relocated to midzone in anaphase ([Figure 3C](#)). CENP-R remained to localize at the centromeres throughout anaphase and telophase, while Aurora B translocated to the midbody from anaphase B to telophase ([Figure 3C](#)). Although our immunofluorescence assay could not detect an exact co-localization between CENP-R and Aurora B, [Broad et al. \(2020\)](#) described Aurora B localization as prominent in the centromere during mitosis and additionally detectable at the outer kinetochore during early mitosis where it phosphorylates substrates to regulate kinetochore–microtubule attachment stability. Thus, we conclude that Aurora B is a binding partner of CENP-R in mitosis.

CENP-R is a bona fide substrate of Aurora B

The spatiotemporal localization and interaction profile of Aurora B with CENP-R in mitosis prompted us to examine their binding interface and inter-relationship. We carried out deletion mutant analyses to pinpoint the region of CENP-R that binds to Aurora B using co-transfection analyses. As shown in [Supplementary Figure S1C](#), both the fragment of aa81–160 and fragment of aa1–140 of CENP-R bound strongly to Aurora B (top IP panel; lanes 3 and 5). To establish a potential enzyme–substrate relationship, we carried out an affinity isolation of the CENP-R-containing protein in mitotic HeLa cells followed by mass spectrometric identification of Aurora B phosphorylation sites in CENP-R. Mitotic HeLa cells treated with hesperadin, an Aurora B inhibitor, was used as a control. Results of the mass spectrometry identified Ser28 and Ser46 as the sites phosphorylated by Aurora B as shown in [Supplementary Table S3](#) ([Supplementary Figure S2A](#)). Critical examination of these two sites revealed that only Ser28 fits Aurora B substrate motif whereas Ser46 fits CDK1 substrate motif. To further confirm the site, we carried out *in vitro* phosphorylation assay and subjected the reaction product to mass spectrometric analyses. Indeed, we identified that Ser28 of recombinant GST-CENP-R was phosphorylated by Aurora B ([Figure 4A](#)). We also demonstrated Ser28 as the main site of CENP-R phosphorylation by Aurora B through an *in vitro* kinase assay with ^{32}P -ATP autoradiograph ([Figure 4B](#)).

Phosphorylation of CENP-R prompted us to examine whether there is functional relevance of Ser28 phosphorylation in mitosis. We introduced GFP-tagged wild-type (WT) and mutated (S28A and S28D) CENP-R constructs together with mCherry-H2B into synchronized HeLa cells deficient of endogenous CENP-R protein and examined their mitotic progression. As shown in [Figure 4C](#), most cells expressing CENP-R-WT progressed from G2 phase into mitotic anaphase within 30 min (top panel). Under the same experimental set-up, the majority of cells expressing non-phosphorylatable mutant CENP-R-S28A progressed from G2 phase into mitotic anaphase within 40 min without apparent

mitotic defects (middle panel). Surprisingly, a large proportion of cells expressing phospho-mimicking mutant CENP-R-S28D were arrested in near-metaphase with apparent chromosome alignment defects ([Figure 4C](#), bottom panel, arrow). A survey of >100 mitotic cells indicated that persistent expression of phospho-mimicking mutant CENP-R resulted in cell arrest in prometaphase or near-metaphase with misaligned chromosomes ([Figure 4D](#)). Also, the proportion of cells with misalignment was moderately elevated in cells expressing CENP-R-S28A. Taken together, we reason that Aurora B-elicited phosphorylation of CENP-R is important in proper metaphase formation and accurate metaphase–anaphase transition during mitosis. Again, the cells expressing CENP-R-S28D were subjected to reversine treatment and arrested in metaphase for >1 h to test whether the SAC was activated. Strikingly, cells expressing CENP-R-S28D mutant in near-metaphase for >1 h proceeded to divide in ~30 min although with defects ([Supplementary Figure S2B](#)). We verified that GFP-tagged CENP-R-WT, CENP-R-S28A, and CENP-R-S28D were expressed in an equal amount in cells with depletion of endogenous CENP-R ([Supplementary Figure S2C](#)). Thus, the expression of CENP-R-S28D causes SAC activation.

Phosphorylation of CENP-R by Aurora B weakens kinetochore–microtubule interactions

To address the underlying mechanism of how Aurora B-elicited phosphorylation towards CENP-R regulation of faithful mitotic progression, we first carefully compared the kinetochore localization patterns of CENP-R-S28A and CENP-R-S28D. As shown in [Figure 5A](#), the intensity of CENP-R-S28A at the centromere was similar to that of CENP-R-WT. However, CENP-R-S28D displayed substantially reduced kinetochore localization compared to CENP-R-WT. Western blotting analyses showed that exogenous CENP-R variants expressed at comparable levels ([Figure 5B](#)). Suppression of CENP-R did not alter the localization of Aurora B to centromeres ([Figure 5C](#); [Supplementary Figure S3A](#)). A survey of centromere intensities of different kinetochore components in CENP-R-S28A/S28D-expressing cells indicated that the Ser28 phosphorylation of CENP-R does not affect the centromere localization of CENP-U and Hec1 ([Figure 5D](#); [Supplementary Figure S3B](#)).

To test the functional activity of microtubule capturing in the cells depleted of CENP-R, we adopted a well-established monastrol washout protocol ([Lampson et al., 2004](#)). If kinetochore microtubule attachment to the centromere are impaired, the bipolar spindle would be formed abnormally. Consistent with our prediction, real-time analyses of control shRNA-treated cells showed that bipolar spindles are efficiently and accurately formed in monastrol-released cells ([Supplementary Figure S4A](#), top panel). However, bipolar spindle formed aberrantly in CENP-R-deficient cells ([Supplementary Figure S4A](#), middle panel). In control shRNA-treated cells, an accurate bipolar spindle formed at 30 min after release from monastrol treatment. However, the bipolar spindle failed to form properly, as judged by chromosome alignment errors at the metaphase equator, even at 80 min after release from monastrol in cells depleted

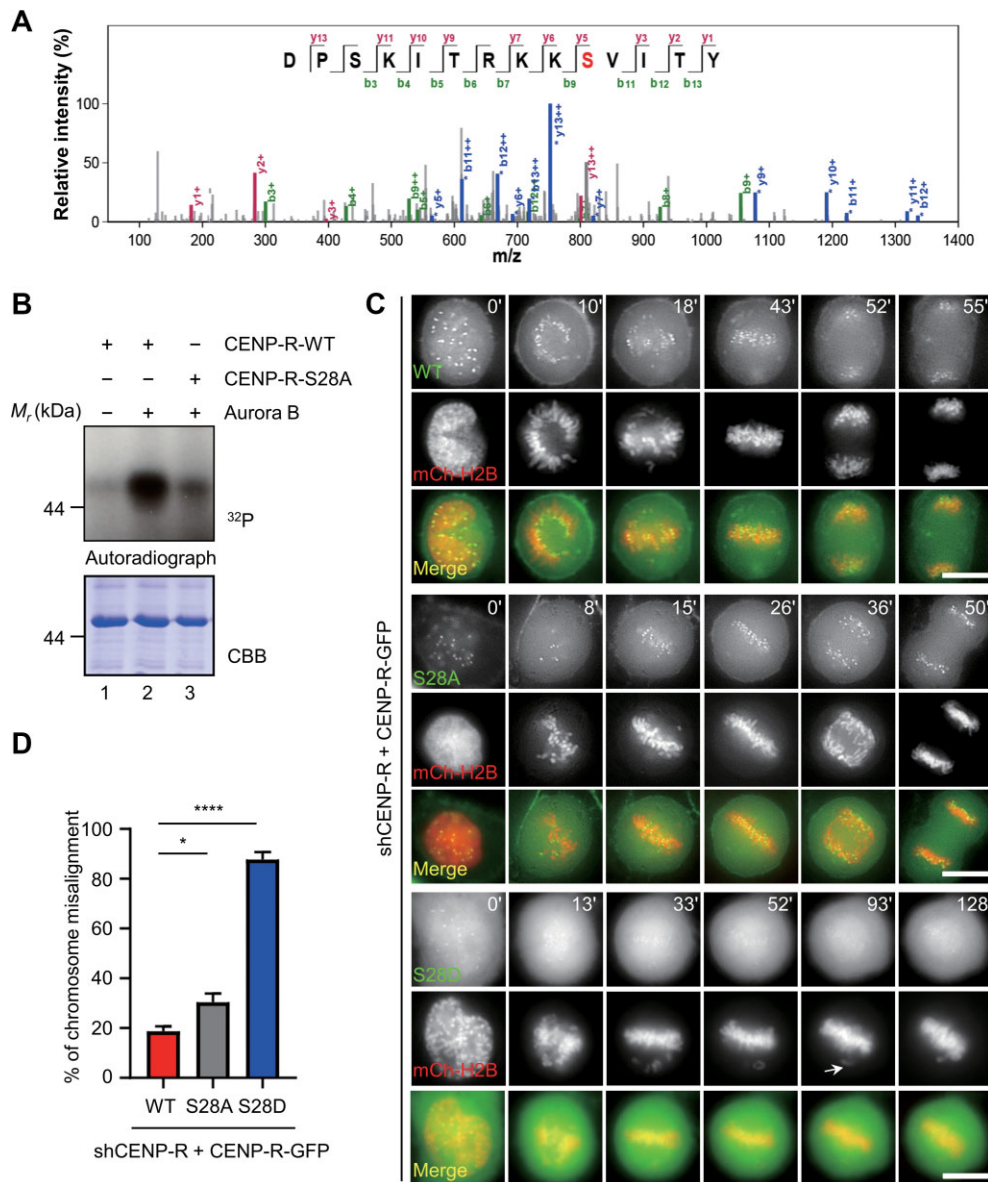


Figure 4 CENP-R is a *bona fide* substrate of Aurora B. **(A)** Mass spectrometric identification of CENP-R Ser28 phosphorylation by Aurora B kinase. **(B)** *In vitro* kinase assay using Aurora B kinase to phosphorylate GST-CENP-R-WT and the S28A mutant. An autoradiograph showing incorporation of radioactive γ - 32 P-ATP (top) and CBB staining of purified proteins (bottom). **(C)** Real-time imaging of chromosome movements in HeLa cells co-transfected with mCherry-H2B and CENP-R-GFP (WT, S28A, and S28D) constructs in the absence of endogenous CENP-R. Chromosomes were marked by mCherry-H2B. Arrow indicates misaligned chromosome. Time is indicated in minutes. Scale bar, 10 μ m. **(D)** Bar graph illustrating percentage of cells with chromosome alignment defects in **C**. An average of 50 GFP- and mCherry-positive mitotic cells from three separate experiments were surveyed. Statistical significance was tested by two-sided *t*-test and represented by * $P < 0.05$ and **** $P < 0.0001$; $n = 3$. Bars indicate mean \pm SD.

of CENP-R (Supplementary Figure S4A, middle panel). Statistical analyses of real-time imaging of chromosome alignment for 60 min after release from monastrol demonstrated that >60% of mitotic cells failed to align chromosomes correctly in CENP-R-deficient cells and >80% of mitotic cells failed to form aligned chromosomes in Aurora B-deficient cells (Supplementary Figure S4A, bottom panel, and Figure S4B). We confirmed that our Aurora B knockdown was potent (Supplementary Figure S4C).

Thus, we speculated that dynamic phosphorylation of CENP-R may be involved in correcting aberrant kinetochore–microtubule attachment.

Previous works reported that recombinant CENP-QU complex exhibits microtubule-binding activity *in vitro* (Amaro et al., 2010; Hua et al., 2011; Pesenti et al., 2018). Since phosphorylation of CENP-R reduces its localization to the centromere, we sought to examine whether CENP-R phosphorylation leads to unstable

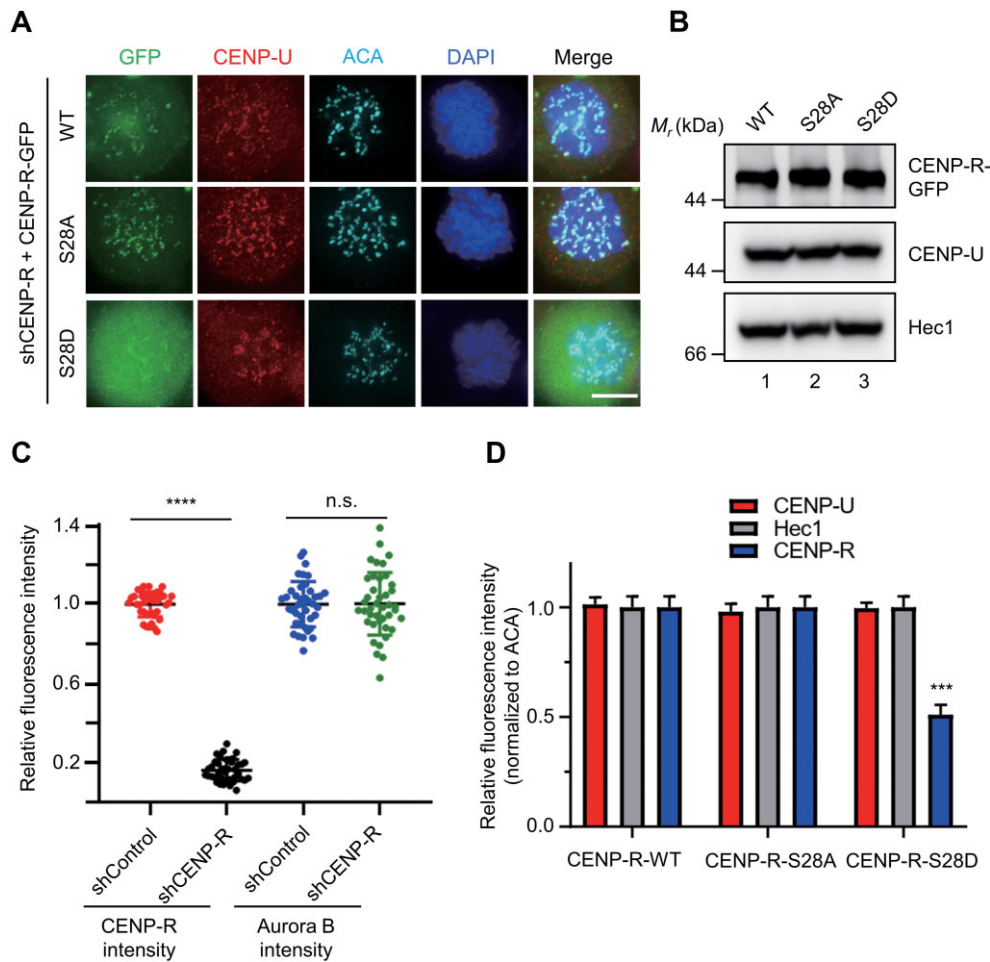


Figure 5 Phosphorylation of CENP-R by Aurora B destabilizes CENP-R localization to the centromere. **(A)** Phosphorylation of CENP-R by Aurora B attenuates the localization of CENP-R to the centromere. HeLa cells were transfected with ShCENP-R along with CENP-R (WT, S28A, and S28D) constructs. At 48 h post transfection, cells were fixed and stained with CENP-U (red), centromere (ACA; cyan), and DAPI (blue). Scale bar, 10 μ m. **(B)** Evaluation of CENP-R, CENP-U, and Hec1 protein expression levels in the experiment shown in **A**. **(C)** Aurora B localization to the centromere is independent of CENP-R, according to the statistical analysis of Aurora B localization in the CENP-R-deficient cells. Statistical significance was tested by two-sided *t*-test and represented by **** $P < 0.0001$; n.s., not significant; $n = 3$. Bars indicate mean \pm SD. **(D)** Statistical analyses of CENP-U and Hec1 intensity at the centromere/kinetochore of CENP-R-GFP-expressing cells (WT, S28A, and S28D). Note that the level of centromere-associated CENP-R-GFP is low in the S28D-expressing cells. An average of 60 mitotic cells from three separate experiments were surveyed. Statistical significance was tested by two-sided *t*-test and represented by *** $P < 0.001$; $n = 3$. Bars indicate mean \pm SD.

kinetochore–microtubule attachment. To this end, we analyzed the inter-kinetochore tension, a readout of kinetochore–microtubule attachment stability, in HeLa cells transfected with shCENP-R or control shRNA. Our previous studies have established that NDC80 and MIS12 complexes are essential for stabilizing kinetochore–microtubule attachments (Liu et al., 2007; Yang et al., 2008). Distance between the sister kinetochores marked by ACA has been used as an accurate reporter for judging the tension developed across the kinetochore pair (Figure 6A, magnified insets). In this case, shortened distance often reflects unstable microtubule attachment to the kinetochore, in which less tension is developed across the sister kinetochore. We measured this distance in 100 kinetochore pairs, in which both

kinetochores were in the same focal plane in both siRNA-treated cells and control cells (Figure 6A and B). As shown in Figure 6A, depletion of CENP-R resulted in errors in chromosome alignment at the equator. Control kinetochores exhibited a separation of $1.61 \pm 0.19 \mu$ m, whereas the distances between kinetochores were $1.25 \pm 0.18 \mu$ m in CENP-R-depleted cells. We further examined the kinetochore fiber in cells depleted of CENP-R. As shown in Supplementary Figure S5A and B, majority of unaligned kinetochore lost microtubule attachment in CENP-R-depleted cells, indicating unstable kinetochore microtubule attachment (Supplementary Figure S5A, d', arrow and magnified inset). On the contrary, kinetochore microtubule attachments were stable in control cells (Supplementary Figure S5A, d, arrow

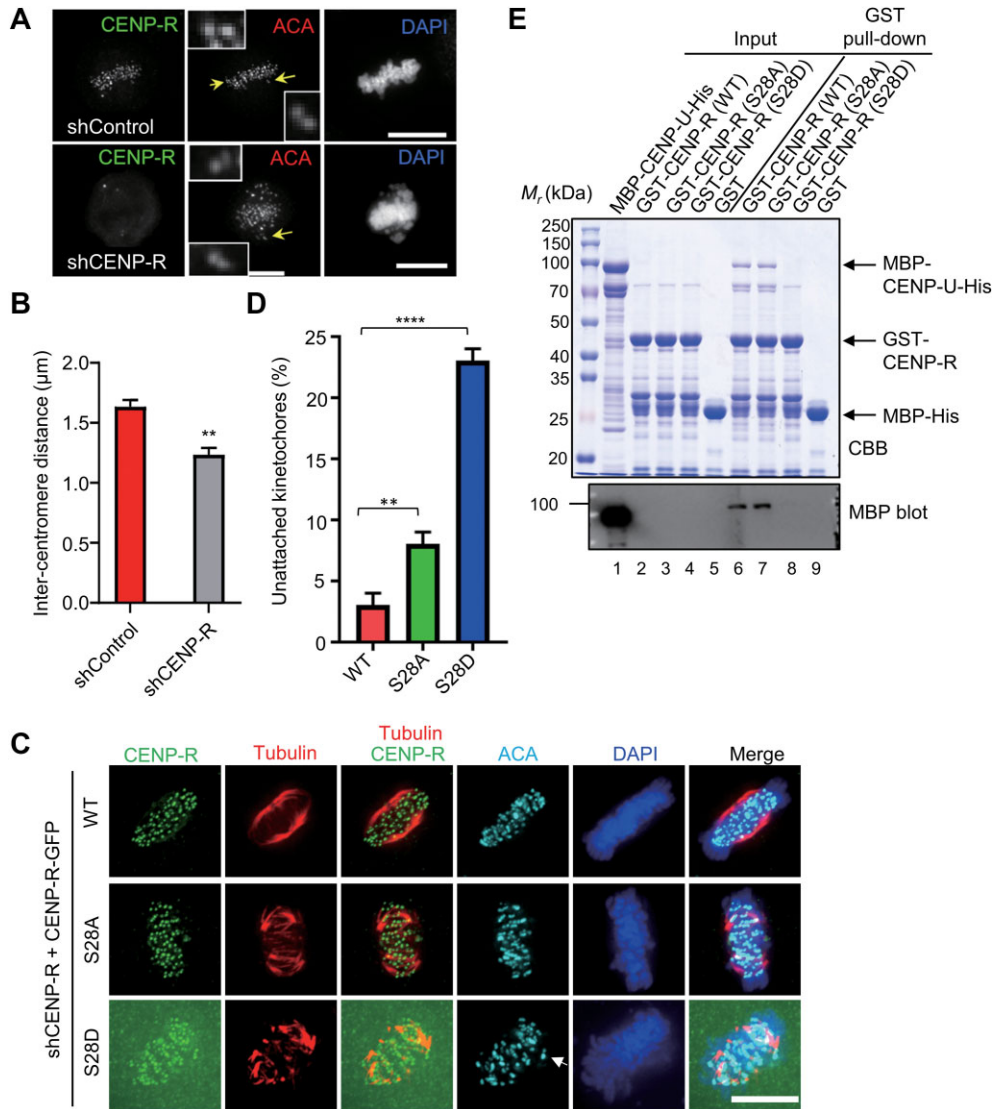


Figure 6 Phosphorylation of CENP-R by Aurora B regulates mitotic spindle plasticity. **(A)** CENP-R is essential for inter-centromere tension during mitotic chromosome segregation. shControl-treated cells and ShCENP-R-treated cells were immuno-stained for centromere (ACA; red), CENP-R (green), and DNA (blue). Note that shRNA suppressed the expression level of CENP-R. Scale bar, 10 μ m. **(B)** Quantitation of inter-centromere distance marked by ACA staining in **A**. Centromere distance is measured between kinetochores that are marked by ACA staining and localized in the same focal plane as described under ‘Materials and methods’. Each value from treated samples was calculated from >100 kinetochores selected from at least 10 different cells. Statistical significance was tested by two-sided *t*-test and represented by $^{***}P < 0.01$; $n = 3$. Bars indicate mean \pm SD. **(C)** Representative images of cells treated with shCENP-R and rescued with CENP-R-GFP (WT, S28A, and S28D). Before fixation, cells were treated with cold DMEM at 4°C for 10 min. Then, cells were fixed and stained for microtubule (red), ACA (cyan), and DNA (blue). Scale bar, 10 μ m. **(D)** Quantification of the level of unaligned kinetochores in cells treated as in **C** (arrow). Bars represent mean \pm SD of three independent experiments. In each experiment, 10 cells were measured (>30 kinetochores per cell). Statistical significance was tested by Student’s *t*-test and represented by $^{**}P < 0.01$ and $^{****}P < 0.0001$. **(E)** *In vitro* pull-down assay of GST-CENP-R (WT, S28A, and S28D) with MBP-CENP-U-His. The gel was stained with CBB (upper panel). Lower panel shows western blotting analysis with anti-His antibody.

and magnified inset). To reveal the underlying mechanism, we subjected HeLa cells expressing GFP-tagged CENP-R-WT, CENP-R-S28A, or CENP-R-S28D to cold treatment and analyzed the binding between the kinetochore and microtubules. As shown in **Figure 6C** (top and middle panels), most kinetochores

correctly bound to microtubules in cells expressing CENP-R-WT or CENP-R-S28A. However, in cells expressing CENP-R-S28D mutant, a significant number of kinetochores completely failed to attach with microtubules (**Figure 6C**, bottom panel, arrow; **Figure 6D**). Taken together, these data demonstrate

that CENP-R might contribute to kinetochore–microtubule attachment stability and the phospho-mimetic S28D mutant causes unstable kinetochore–microtubule attachment.

Previous studies have demonstrated that the kinetochore localization of CENP-R depends on its binding with CENP-QU (Pesenti et al., 2018). If Aurora B phosphorylation of CENP-R disrupts the kinetochore association of CENP-R, it is likely that phosphorylation of Ser28 weakens the binding between CENP-R and CENP-QU. To verify this prediction, aliquots of CENP-R-GFP (WT, S28A, and S28D) constructs were transiently transfected to express the respective proteins. Twenty-four hours after transfection, the transfected cells were prepared for generating clarified cell lysates followed by immunoprecipitation. As shown in Supplementary Figure S5C, immunoprecipitation of CENP-R-WT and CENP-R-S28A brought down CENP-U (lanes 4 and 6). However, CENP-R-S28D could not pull down CENP-U (lane 5) *in vivo*. To further confirm the interaction between CENP-R and CENP-U *in vitro*, we used affinity matrix to pull down CENP-U. As shown in Figure 6E (lane 8), GST-CENP-R-S28D could not pull down CENP-U, which further confirms the results of our earlier experiments. Thus, we conclude that Aurora B phosphorylation towards CENP-R dynamically liberates CENP-R from CENP-U binding and this may be necessary to correct aberrant kinetochore microtubule attachment to ensure accurate chromosome segregation.

Discussion

We have identified that CENP-R, a subunit of CCAN, physically interacts with Aurora B *in vitro* and *in vivo*. Our functional analyses demonstrate that CENP-R is a *bona fide* substrate of Aurora B and its phosphorylation is required for stable kinetochore–microtubule attachment. Interestingly, phosphorylation of CENP-R weakens its localization to the kinetochore and results in unstable kinetochore–microtubule interaction. However, depletion of CENP-R does not affect the kinetochore localization of CENP-A, CENP-B, Hec1, Aurora B, or components of CENP-HIKM (Pesenti et al., 2018), supporting the functional importance of CENP-R as a fine-tuning subunit. Our study identifies CENP-R as a previously unrecognized substrate of Aurora B and suggests that the phosphorylation of CENP-R, in addition to other substrates, may be responsible for error-correction of aberrant kinetochore–microtubule attachments by the kinase (Figure 7). Previous studies have also reported the phosphorylation of CENP-R at Ser28 by Pak1 with co-activator and apoptosis activity (Talukder et al., 2008; Das et al., 2014). However, it was unclear whether CENP-R can be phosphorylated by other mitotic kinases and whether phosphorylation of CENP-R exhibits a context-dependent function in mitosis.

Establishing correct kinetochore–microtubule attachment is the precondition of faithful mitosis. The NDC80 complex is extensively investigated as the main microtubule receptor at outer kinetochore (Cheeseman et al., 2006; DeLuca et al., 2006). In addition, the astrin–SKAP complex and Ska1/2/3 complex selectively localize to the kinetochores with correct microtubule attachment to stabilize the linkage (Fang et al., 2009;

Schmidt et al., 2010; Chan et al., 2012; Zhang et al., 2021). Besides the aforementioned complex, the CENP-OPQUR complex is reported to have microtubule-binding activity (Pesenti et al., 2018). Our previous finding of CENP-U–Hec1 interaction provides a novel link between spindle microtubules and the kinetochore core complex via CCAN (Hua et al., 2011). In fact, CENP-Q and CENP-U have been established as microtubule-binding proteins (Hua et al., 2011; Pesenti et al., 2018).

One outstanding question in the field is how CENP-R functions in mitosis, as CENP-R is absent from lower eukaryotic cells such as yeast. Here, we propose that upon phosphorylation, CENP-R detaches from the kinetochore due to weakened binding between CENP-U and CENP-R. Due to the loss of CENP-R, kinetochore–microtubule attachment stability is decreased, and hence the wrong attachments are released and the new attachments are re-established (Figure 7).

It would be of great interest to delineate the precise molecular interaction underlying the Aurora B–CENP-R–CENP-U subcomplex assembly *in vitro* and examine how perturbation of such an interaction alters the plasticity of kinetochore assembly and chromosome segregation by a combination of nanometer-resolution distribution of single molecules with photo-activatable fluorescent proteins in living dividing cells (Xia et al., 2014).

In this study, we identified CENP-R as a *bona fide* substrate of Aurora B. The phospho-mimetic CENP-R-S28D mutant causes massive chromosome misalignment, while the non-phosphorylatable CENP-R-S28A mutant causes elevated proportion of cells with chromosome alignment defects. Mechanistically, persistent CENP-R phosphorylation by Aurora B destabilizes kinetochore microtubule attachment because of disrupted CENP-U–CENP-R binding. Our studies reveal how dynamic phosphorylation of CENP-R ensures accurate sister chromatid separation.

Materials and methods

Plasmids, shRNA, and transfection

The WT human CENP-R construct was generated by recombination method whereby both CENP-R gene and the vector pEGFP-N1 were amplified by polymerase chain reaction (PCR) and recombined according to Vazyme C214 user manual. GST, pPET-22b, and all other plasmids used in this work were constructed similarly as stated above. All site and deletion mutants of CENP-R were generated by PCR-based mutagenesis approach. The three CENP-R shRNAs used were generated by inserting CENP-R shRNA sequences behind the hPGK promoter of pLKO.1 vector. The nucleotide sequences for shRNA against CENP-R were taken from the first three sequences used by Pesenti et al. (2018): 5′-GAAGUUGGAUGGUCUGUUA-3′ (designated as shCENP-R #1), 5′-UGACAGCUAUGAAUCCUU-3′ (designated as shCENP-R #2), and 5′-UAAGUAGUAUCAGGCCUUU-3′ (designated as shCENP-R #3). To increase the transduction efficiency, the RNA-containing lentiviral plasmid was then co-transfected with two packing plasmids psPAX2 and pMD2.G into human embryonic kidney 293T (HEK293T) cells to generate

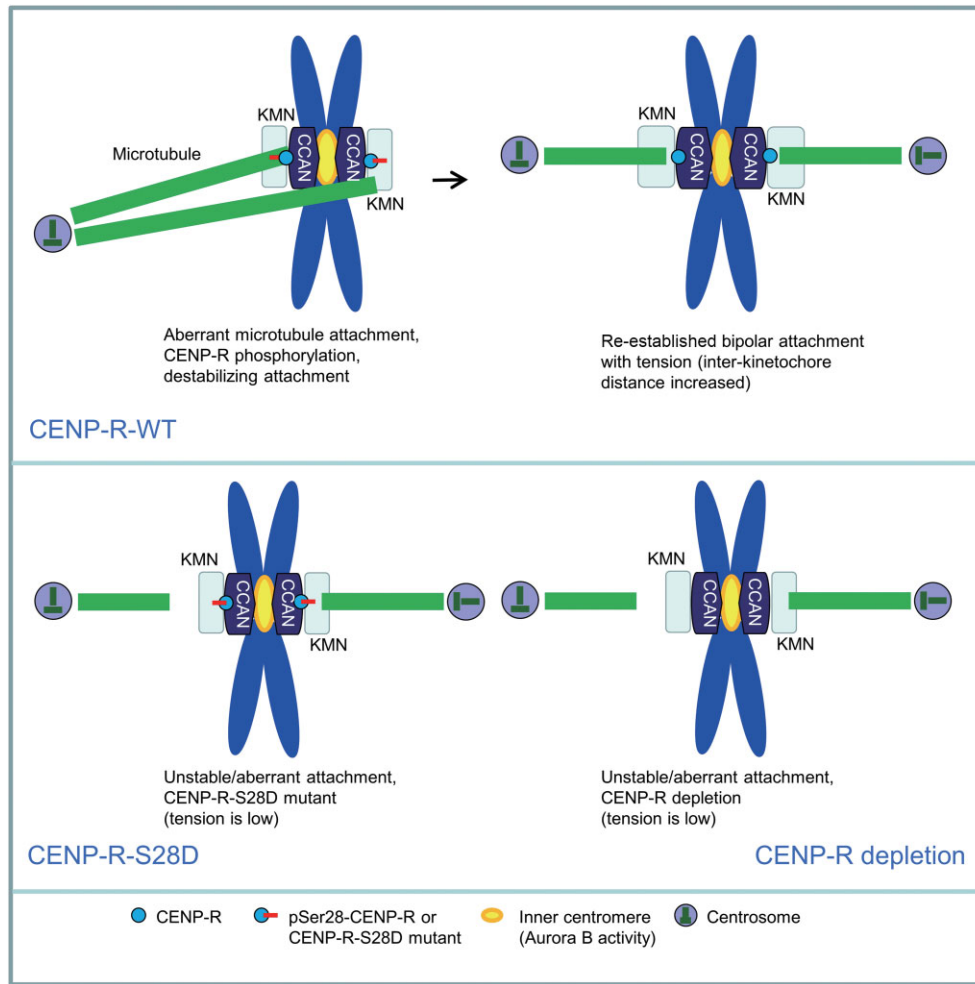


Figure 7 Working model accounting for function of Aurora B phosphorylation of CENP-R in the kinetochore–microtubule attachment. During prometaphase, when the aberrant kinetochore microtubule attachment is detected, Aurora B phosphorylates CENP-R. Then, phosphorylated CENP-R detaches from kinetochore–microtubule binding interface. The wrong attachments are corrected and the cell re-establishes correct bipolar attachment with proper tension. On the contrary, when phospho-mimetic CENP-R-S28D mutant is persistently expressed, the kinetochore–microtubule attachments are unstable. The correct attachment with tension cannot be established. In the scenario of CENP-R depletion, the kinetochore–microtubule attachments are also unstable. Both expression of CENP-R-S28D and depletion of CENP-R cause chronic activation of the SAC.

lentivirus. HeLa cells were transduced with the lentivirus for 48 h and were subjected to puromycin selection at 0.3 $\mu\text{g/ml}$ for 3 days to obtain stable CENP-R knockdown cell lines. The control shRNA was generated in the same manner. All the plasmids and shRNAs were transfected into cells using Lipofectamine 2000 or Lipofectamine 3000 (Invitrogen) according to the user's manual. The packaged viruses were then used to transduce the cells used in this work whenever required.

Cell culture, synchronization, and drug treatments

HEK293T and HeLa cells were routinely maintained in advanced Dulbecco's Modified Eagle's Medium (DMEM; Invitrogen) with 10% (v/v) fetal bovine serum (FBS; HyClone) and 100 units/ml of penicillin plus 100 $\mu\text{g/ml}$ streptomycin (Gibco). To enrich mitotic cells, HeLa cells were treated with

2.5 mM thymidine (Invitrogen) for 14 h and then released into a fresh DMEM. For monastrol (50 μM , Sigma) treatment, the drug was added into the culture medium 8 h after release and maintained for 2 h. Metaphase HeLa cells for quantification of chromosome misalignment were enriched with MG132 (20 μM , Sigma) treatment. For immunoprecipitation of GFP-tagged proteins, HeLa cells were treated with nocodazole (0.1 $\text{ng}/\mu\text{l}$) for 14 h and then harvested for experiments. For Hesperadin (100 nM, Sigma) treatment, the drug was added into the culture medium and maintained for 30 min.

Immunofluorescence microscopy, image processing, and quantification

For other immunofluorescence experiments, HeLa cells grown on coverslips were fixed and permeabilized simultaneously with

PTEM buffer (50 mM Pipes, pH 6.8, 0.2% Triton X-100, 10 mM EGTA, 1 mM MgCl₂, and 4% formaldehyde) at room temperature, then blocked with phosphate-buffered saline with 0.05% Tween-20 (PBST) buffer containing 1% bovine serum albumin (Sigma) for 30 min at room temperature, and sequentially incubated with the primary and secondary antibodies followed by DNA staining with DAPI (Sigma). Imaging of samples was performed on DeltaVision microscope (Applied Precision) with a 60× objective lens, NA = 1.42, with optical sections acquired 0.25 μm apart in the z-axis. The original deconvoluted images taken from a specific focal plane were projected into one image with the help of Softworx (Applied Precision). The 16-bit gray-scale images were acquired from pictures taken with the same exposure time within each experiment. The images were exported into 24-bit RGB images using Adobe Photoshop after deconvolution. Identically scaled images are shown in the same panel. ImageJ (rsb.info.nih.gov/ij/) was used to measure the kinetochore intensities of non-deconvoluted images. The levels of kinetochore-associated proteins were quantified as previously described (Dou et al., 2015). Briefly, the ground pixel intensities were measured and subtracted from the average pixel intensities from a minimum of 100 kinetochore pairs from five cells. Stained ACA was used to normalize the pixel intensities at each kinetochore pair to make up for any changes in staining or image acquisition. Unless stated differently, the values of the untreated cells were plotted as controls with the treated group plotted against them. The Applied Precision Software was used for deconvolution and z-stack projection, and finally images were processed with Adobe Photoshop. ImageJ software was used for all colocalization analyses and fluorescence intensity measurements.

To classify cells with misaligned chromosome, an automated analysis was employed as described previously (Gama Braga et al., 2021). The standard/control used were the cells arrested at metaphase, and the distance between the two spindle poles in the control cells was accurately measured. An alignment region was then established based on the area between the two spindle poles and used as the benchmark in determining misaligned chromosomes. Kinetochores falling outside the alignment region are considered mis-aligned. Each set of experiment or cell line has its own control/standard.

Live cell imaging

For Live cell imaging, HeLa cells were maintained in glass-bottom culture dishes (MatTek) and cultured at 37°C in CO₂-independent medium (Gibco) supplemented with 10% (v/v) FBS and 2 mM glutamine. Images were acquired at 2- or 3-min intervals for mitotic cells by a DeltaVision deconvolution microscope system built on an Olympus IX-71 inverted microscope base (Applied Precision). For imaging, a 60× 1.42 NA lens was used, and optical sections were taken at intervals of 0.2 μm. Images for display were generated by projecting single optical sections as described previously (Mo et al., 2016). Images were prepared for publication using Adobe Photoshop software.

Antibodies

Rabbit anti-CENP-R (10743-1-AP, Proteintech), mouse anti-tubulin (3873, Cell Signaling Technology), rabbit anti-GFP (50430-2-AP, Proteintech), mouse anti-His tag (23665, Cell Signaling Technology), mouse anti-FLAG (F3165, Sigma), anti-Cyclin B1 (12231, Cell Signaling Technology), anti-Hec1 (AB3613, Abcam), anti-Aurora B (611082, BD), anti-CENP-U (HPA022048, Atlas), and human anti-centromere auto-antibody (ACA, HCT-0100, Immunovision) were obtained commercially. For all western blotting, signals were detected using HRP-conjugated anti-mouse or anti-rabbit antibodies (Pierce).

Recombinant protein preparation and purification

GST-CENP-R, 6× His-Aurora B, GST plasmids were transformed into *Escherichia coli* strain Rosetta (DE3), and protein expression was induced at a standard cell density (optical density ~0.6) with 0.2 mM IPTG at 16°C for 20 h. Bacteria expressing 6× His-Aurora B was lysed by sonication in Ni-NTA binding buffer (50 mM NaH₂PO₄, pH 8.0, 300 mM NaCl, and 10 mM imidazole) and incubated with Ni-NTA agarose (Qiagen) for 2 h at 4°C. The agarose was washed three times in Ni-NTA binding buffer supplemented with 30 mM imidazole and eluted with Ni-NTA binding buffer supplemented with 250 mM imidazole. Bacterially expressed recombinant proteins of GST-CENP-R and GST were lysed by sonication in PBS buffer supplemented with 0.1% Triton X-100 and incubated with glutathione-Sepharose 4B (GE Healthcare Life Science) for 2 h at 4°C. GST-CENP-R and GST protein were eluted with 20 mM glutathione when necessary or kept on the beads for further assay. All purification procedures were performed at 4°C, and a protease inhibitor cocktail (Sigma) was added to prevent protein degradation.

Immunoprecipitation and pull-down assay

For immunoprecipitation, HEK293T cells expressing 3× FLAG-tagged Aurora B, CENP-R-GFP (and all deletion mutants), and GFP were lysed in IP buffer (50 mM HEPES, 150 mM NaCl, and 2 mM EDTA, pH 7.4) supplemented with 0.1% Triton X-100 plus protease inhibitor cocktail and incubated with anti-FLAG M2 resin for 3 h followed by washing three times with IP buffer. The FLAG-M2 beads were then resolved by sodium dodecyl sulfate–polyacrylamide gel electrophoresis (SDS–PAGE) and immunoblotted with anti-FLAG-tag and anti-GFP-tag antibodies. For anti-GFP immunoprecipitation, the HeLa cells transfected with CENP-R-GFP (plus mutants) were lysed in IP buffer (50 mM Tris-HCl, 150 mM KCl, and 1 mM EDTA, pH 7.4) supplemented with 0.1% Triton X-100 plus protease inhibitor cocktail and immunoprecipitated with GFP-Trap Agarose beads (gta-20, ChromoTek). The binding fractions were analyzed by western blotting with anti-GFP and anti-tubulin antibodies used to stain the membranes.

The pull-down assay with purified GST-CENP-R and 6× His-Aurora B was performed as previously described (Xu et al., 2021). GST-CENP-R purified on glutathione beads were used as an affinity matrix for absorbing 6× His-tagged Aurora B in the buffer containing PBS, pH 7.4, 0.1% Triton X-100, and 1 mM

PMSF for 3 h at 4°C. The beads were washed three times with PBS plus 0.1% Triton X-100 and once with PBS and then boiled for 5 min in SDS–PAGE sample buffer. Proteins were resolved by SDS–PAGE for Coomassie Brilliant Blue staining and western blotting.

In vitro kinase assay

In vitro kinase assay was performed as previously reported (Yu et al., 2020). 6× His-tagged Aurora B kinase was expressed in bacteria and purified by Ni²⁺-nitrilotriacetic acid beads. The kinase reactions were performed in 40 μl 1× kinase buffer (25 mM Tris, pH 7.5, 10 mM MgCl₂, 1 mM DTT, and 1 mM EGTA) containing 1 μl eluted Aurora B kinase, 5 μl GST-CENP-R on sepharose beads, and 200 μM ATP plus 5 μCi γ-³²P-ATP. The mixtures were incubated at 30°C for 30 min. The reactions were stopped with 5× SDS sample buffer, and the sample was separated by SDS–PAGE and stained with Coomassie Brilliant Blue.

Mass spectrometric sample preparation and analyses

The GFP immunoprecipitation and *in vitro* kinase assay were conducted as described above. The sample was reduced with 10 mM DTT in 50 mM ammonium bicarbonate at 56°C for 45 min and then alkylated with 30 mM iodoacetamide for 30 min in dark. After the above process, 2 μg of α-chymotrypsin (Proxino, HLS CHY001C) was added to the *in vitro* kinase assay sample for overnight digestion at 30°C, and 2 μg of trypsin (Promega, V5111) was added to GFP immunoprecipitation sample for overnight digestion at 37°C. After digestion, the peptide sample was desalted and analyzed with Thermo Fisher Q Exactive plus and Orbitrap Exploris 480 mass spectrometer equipped with Easy-nanoLC 1200. The raw file was analyzed with pFind Studio 3 and PD2.5. The human database was from Uniprot (Proteome ID: UP000005640). Phosphorylation (S/T, +79.9663 Da) and oxidation (M, +15.9949 Da) modifications were included as variable modification. Carbamidomethyl (C, +57.0215 Da) was set as fix modification.

For an interest to identify true CENP-R binders, our mass spectrometric analyses of *bona fide* interactors for CENP-R involved an initial search of CARPome, a contaminant repository for affinity purification, to eliminate background contaminants such as proteins bound to epitope tag (Mellacheruvu et al., 2013). Since the negative controls in CARPome are largely bait-independent, this database search prompted our characterization of true CENP-R-interacting proteins.

Statistics

All statistics were described in the figure legends. The student's *t*-test was applied for experimental comparisons, using GraphPad Prism 7.

Supplementary material

Supplementary material is available at *Journal of Molecular Cell Biology* online.

Funding

This work was supported by the Ministry of Science and Technology of China (MOST) grants (2017YFA0503600), the National Natural Science Foundation of China (NSFC) grants (91854203, 31621002, 91853115, 21922706, 92153302, 32090040, 22177106, 31871359, 92053104, 32100612, 22137007, and 31970655), the Ministry of Education (IRT_17R102, 20113402130010, and YD2070006001) Strategic Priority Research Program of the Chinese Academy of Sciences (XDB19040000), Anhui Provincial Natural Science Foundation Grant (2108085J15 and 1908085MC64), and the Fundamental Research Funds for the Central Universities (WK2070000066 and WK2070000194).

Conflict of interest: none declared.

Author contributions: X. Yao and Xing Liu conceived the project. D.M.S. performed most biochemical experiments and cell biological characterization. M.M. conducted immunoprecipitation assay. X. Yuan and Z.D. performed *in vivo* phosphorylation site identification and *in vivo* CENP-R-binding protein identification using mass spectrometric analyses. X.G., U.E., D.W., T.Y., and Z.W. conducted immunofluorescence analyses and data analyses. Xu Liu, X.S., Y.-C.T., W.P., and P.Z. contributed reagents. D.M.S., Xing Liu, and X. Yao wrote the manuscript, X. Yuan and Z.D. participated in revision, and all authors have read and approved the manuscript.

References

- Amaro, A.C., Samora, C.P., Holtackers, R., et al. (2010). Molecular control of kinetochore–microtubule dynamics and chromosome oscillations. *Nat. Cell Biol.* 12, 319–329.
- Broad, A.J., DeLuca, K.F., and DeLuca, J.G. (2020). Aurora B kinase is recruited to multiple discrete kinetochore and centromere regions in human cells. *J. Cell Biol.* 219, e201905144.
- Cao, B., Zhao, C., Zhang, Y., et al. (2021). The novel interaction mode among centromere sub-complex CENP-O/P/U/Q/R. *J. Mol. Recognit.* 34, e2892.
- Carmena, M., Wheelock, M., Funabiki, H., et al. (2012). The chromosomal passenger complex (CPC): from easy rider to the godfather of mitosis. *Nat. Rev. Mol. Cell Biol.* 13, 789–803.
- Chan, Y.W., Jeyapragash, A.A., Nigg, E.A., et al. (2012). Aurora B controls kinetochore–microtubule attachments by inhibiting Ska complex–KMN network interaction. *J. Cell Biol.* 196, 563–571.
- Cheeseman, I.M., Chappie, J.S., Wilson-Kubalek, E.M., et al. (2006). The conserved KMN network constitutes the core microtubule-binding site of the kinetochore. *Cell* 127, 983–997.
- Cheeseman, I.M., and Desai, A. (2008). Molecular architecture of the kinetochore–microtubule interface. *Nat. Rev. Mol. Cell Biol.* 9, 33–46.
- Cleveland, D.W., Mao, Y., and Sullivan, K.F. (2003). Centromeres and kinetochores: from epigenetics to mitotic checkpoint signaling. *Cell* 112, 407–421.
- Das, S., Yeung, K.T., Mahajan, M.A., et al. (2014). Fas activated serine–threonine kinase domains 2 (FASTKD2) mediates apoptosis of breast and prostate cancer cells through its novel FAST2 domain. *BMC Cancer* 14, 852.
- DeLuca, J.G., Gall, W.E., Ciferri, C., et al. (2006). Kinetochore microtubule dynamics and attachment stability are regulated by Hec1. *Cell* 127, 969–982.
- Ding, X., Deng, H., Wang, D., et al. (2010). Phospho-regulated ACAP4–Ezrin interaction is essential for histamine-stimulated parietal cell secretion. *J. Biol. Chem.* 285, 18769–18780.

- Dou, Z., Liu, X., Wang, W., et al. (2015). Dynamic localization of Mps1 kinase to kinetochores is essential for accurate spindle microtubule attachment. *Proc. Natl Acad. Sci. USA* 112, E4546–E4555.
- Dransfield, D.T., Bradford, A.J., Smith, J., et al. (1997). Ezrin is a cyclic AMP-dependent protein kinase anchoring protein. *EMBO J.* 16, 35–43.
- Fang, L., Seki, A., and Fang, G. (2009). SKAP associates with kinetochores and promotes the metaphase-to-anaphase transition. *Cell Cycle* 8, 2819–2827.
- Fang, Z., Miao, Y., Ding, X., et al. (2006). Proteomic identification and functional characterization of a novel ARF6 GTPase-activating protein, ACAP4. *Mol. Cell. Proteomics* 5, 1437–1449.
- Foltz, D.R., Jansen, L.E., Black, B.E., et al. (2006). The human CENP-A centromeric nucleosome-associated complex. *Nat. Cell Biol.* 8, 458–469.
- Gama Braga, L., Prifti, D.K., Garand, C., et al. (2021). A quantitative and semi-automated method for determining misaligned and lagging chromosomes during mitosis. *Mol. Biol. Cell* 32, 880–891.
- Gascoigne, K.E., Takeuchi, K., Suzuki, A., et al. (2011). Induced ectopic kinetochore assembly bypasses the requirement for CENP-A nucleosomes. *Cell* 145, 410–422.
- Gui, P., Sedzro, D.M., Yuan, X., et al. (2020). Mps1 dimerization and multisite interactions with Ndc80 complex enable responsive spindle assembly checkpoint signaling. *J. Mol. Cell Biol.* 12, 486–498.
- Hori, T., Amano, M., Suzuki, A., et al. (2008). CCAN makes multiple contacts with centromeric DNA to provide distinct pathways to the outer kinetochore. *Cell* 135, 1039–1052.
- Hua, S., Wang, Z., Jiang, K., et al. (2011). CENP-U cooperates with Hec1 to orchestrate kinetochore–microtubule attachment. *J. Biol. Chem.* 286, 1627–1638.
- Kops, G., Snel, B., and Tromer, E.C. (2020). Evolutionary dynamics of the spindle assembly checkpoint in eukaryotes. *Curr. Biol.* 30, R589–R602.
- Lampson, M.A., Renduchitala, K., Khodjakov, A., et al. (2004). Correcting improper chromosome–spindle attachments during cell division. *Nat. Cell Biol.* 6, 232–237.
- Lara-Gonzalez, P., Pines, J., and Desai, A. (2021). Spindle assembly checkpoint activation and silencing at kinetochores. *Semin. Cell Dev. Biol.* 117, 86–98.
- Li, D., Desai-Yajnik, V., Lo, E., et al. (1999). NRIF3 is a novel coactivator mediating functional specificity of nuclear hormone receptors. *Mol. Cell. Biol.* 19, 7191–7202.
- Li, D., Wang, F., and Samuels, H.H. (2001). Domain structure of the NRIF3 family of coregulators suggests potential dual roles in transcriptional regulation. *Mol. Cell. Biol.* 21, 8371–8384.
- Liu, D., Ding, X., Du, J., et al. (2007). Human NUF2 interacts with centromere-associated protein E and is essential for a stable spindle microtubule–kinetochore attachment. *J. Biol. Chem.* 282, 21415–21424.
- Liu, X., Liu, X., Wang, H., et al. (2020). Phase separation drives decision making in cell division. *J. Biol. Chem.* 295, 13419–13431.
- McKinley, K.L., and Cheeseman, I.M. (2016). The molecular basis for centromere identity and function. *Nat. Rev. Mol. Cell Biol.* 17, 16–29.
- Mellacheruvu, D., Wright, Z., and Couzens, A.L. (2013). The CRAPome: a contaminant repository for affinity purification–mass spectrometry data. *Nat. Methods* 10, 730–736.
- Meraldi, P., Draviam, V.M., and Sorger, P.K. (2004). Timing and checkpoints in the regulation of mitotic progression. *Dev. Cell* 7, 45–60.
- Mo, F., Zhuang, X., Liu, X., et al. (2016). Acetylation of Aurora B by TIP60 ensures accurate chromosomal segregation. *Nat. Chem. Biol.* 12, 226–232.
- Musacchio, A., and Desai, A. (2017). A molecular view of kinetochore assembly and function. *Biology* 6, 5.
- Okada, M., Cheeseman, I.M., Hori, T., et al. (2006). The CENP-H–I complex is required for the efficient incorporation of newly synthesized CENP-A into centromeres. *Nat. Cell Biol.* 8, 446–457.
- Pesenti, M.E., Prumbaum, D., Auckland, P., et al. (2018). Reconstitution of a 26-subunit human kinetochore reveals cooperative microtubule binding by CENP-OPQR and NDC80. *Mol. Cell* 71, 923–939.e10.
- Pesenti, M.E., Raisch, T., Conti, D., et al. (2022). Structure of the human inner kinetochore CCAN complex and its significance for human centromere organization. *Mol. Cell* 82, 2113–2131.e8.
- Santaguida, S., Tighe, A., D’Alise, A.M., et al. (2010). Dissecting the role of MPS1 in chromosome biorientation and the spindle checkpoint through the small molecule inhibitor reversine. *J. Cell Biol.* 190, 73–87.
- Schleiffer, A., Maier, M., Litos, G., et al. (2012). CENP-T proteins are conserved centromere receptors of the Ndc80 complex. *Nat. Cell Biol.* 14, 604–613.
- Schmidt, J.C., Kiyomitsu, T., Hori, T., et al. (2010). Aurora B kinase controls the targeting of the Astrin–SKAP complex to bioriented kinetochores. *J. Cell Biol.* 191, 269–280.
- Talukder, A.H., Li, D.Q., Manavathi, B., et al. (2008). Serine 28 phosphorylation of NRIF3 confers its co-activator function for estrogen receptor- α transactivation. *Oncogene* 27, 5233–5242.
- Tian, T., Chen, L., Dou, Z., et al. (2022). Structural insights into human CCAN complex assembled onto DNA. *Cell Discov.* 8, 90.
- van der Waal, M.S., Hengeveld, R.C., van der Horst, A., et al. (2012). Cell division control by the chromosomal passenger complex. *Exp. Cell Res.* 318, 1407–1420.
- Wang, H., Hu, X., Ding, X., et al. (2004). Human Zwint-1 specifies localization of Zeste White 10 to kinetochores and is essential for mitotic checkpoint signaling. *J. Biol. Chem.* 279, 54590–54598.
- Xia, P., Liu, X., Wu, B., et al. (2014). Superresolution imaging reveals structural features of EB1 in microtubule plus-end tracking. *Mol. Biol. Cell* 25, 4166–4173.
- Xu, L., Ali, M., Duan, W., et al. (2021). Feedback control of PLK1 by Apolo1 ensures accurate chromosome segregation. *Cell Rep.* 36, 109343.
- Yan, K., Yang, J., Zhang, Z., et al. (2019). Structure of the inner kinetochore CCAN complex assembled onto a centromeric nucleosome. *Nature* 574, 278–282.
- Yang, Y., Wu, F., Ward, T., et al. (2008). Phosphorylation of HsMis13 by Aurora B kinase is essential for assembly of functional kinetochore. *J. Biol. Chem.* 283, 26726–26736.
- Yatskevich, S., Muir, K.W., Bellini, D., et al. (2022). Structure of the human inner kinetochore bound to a centromeric CENP-A nucleosome. *Science* 376, 844–852.
- Yu, R., Wu, H., Ismail, H., et al. (2020). Methylation of PLK1 by SET7/9 ensures accurate kinetochore–microtubule dynamics. *J. Mol. Cell Biol.* 12, 462–476.
- Zhang, M., Yang, F., Wang, W., et al. (2021). SKAP interacts with Aurora B to guide end-on capture of spindle microtubules via phase separation. *J. Mol. Cell Biol.* 13, 841–852.